

OMNIQUANT: OMNIDIRECTIONALLY CALIBRATED QUANTIZATION FOR LARGE LANGUAGE MODELS

Wenqi Shao^{†1}, Mengzhao Chen^{†1}, Zhaoyang Zhang³, Peng Xu^{1,2}, Lirui Zhao,
Zhiqian Li², Kaipeng Zhang¹, Peng Gao¹, Yu Qiao¹, Ping Luo^{*1,2}

¹OpenGVLab, Shanghai AI Laboratory ²The University of Hong Kong

³The Chinese University of Hong Kong

ABSTRACT

Large language models (LLMs) have revolutionized natural language processing tasks. However, their practical deployment is hindered by their immense memory and computation requirements. Although recent post-training quantization (PTQ) methods are effective in reducing memory footprint and improving the computational efficiency of LLM, they hand-craft quantization parameters, which leads to low performance and fails to deal with extremely low-bit quantization. To tackle this issue, we introduce an Omnidirectionally calibrated Quantization (**OmniQuant**) technique for LLMs, which achieves good performance in diverse quantization settings while maintaining the computational efficiency of PTQ by efficiently optimizing various quantization parameters. OmniQuant comprises two innovative components including Learnable Weight Clipping (LWC) and Learnable Equivalent Transformation (LET). LWC modulates the extreme values of weights by optimizing the clipping threshold. Meanwhile, LET tackles activation outliers by shifting the challenge of quantization from activations to weights through a learnable equivalent transformation. Operating within a differentiable framework using block-wise error minimization, OmniQuant can optimize the quantization process efficiently for both weight-only and weight-activation quantization. For instance, the LLaMA-2 model family with the size of 7-70B can be processed with OmniQuant on a single A100-40G GPU within 1-16 hours using 128 samples. Extensive experiments validate OmniQuant’s superior performance across diverse quantization configurations such as W4A4 (4-bit weight, 4-bit activation), W6A6, W4A16, W3A16, and W2A16. Additionally, OmniQuant demonstrates effectiveness in instruction-tuned models and delivers notable improvements in inference speed and memory reduction on real devices. Codes and models are available at <https://github.com/OpenGVLab/OmniQuant>.

1 INTRODUCTION

Large language models (LLMs) such as GPT-4 (Bubeck et al. (2023)) and LLaMA (Touvron et al. (2023a)), have demonstrated impressive performance across various natural language benchmarks (Hendrycks et al. (2020); Bisk et al. (2020); Zellers et al. (2019)). Furthermore, the language understanding capabilities inherent in LLMs can be successfully transferred into multimodal models (Mu et al. (2023); Xu et al. (2023); Zhang et al. (2023)). Thereby, LLMs can be regarded as precursors to artificial general intelligence (Bubeck et al. (2023)). However, the considerable computational and memory requirements of LLMs pose substantial challenges. For instance, the GPT-3 model (Brown et al. (2020)) requires 350G of memory to load its parameters in FP16 format, which corresponds to the requirement of at least five A100-80G GPUs for inference. This significant demand for computational resources and associated communication overheads impedes the practical deployment of LLMs in real-world applications.

Quantization has shown to be promising to mitigate both computational and memory overhead in LLMs. In general, it comes in two types including post-training quantization (PTQ) and

*Corresponding author: Ping Luo, pluo@cs.hku.edu

† Equal Contribution

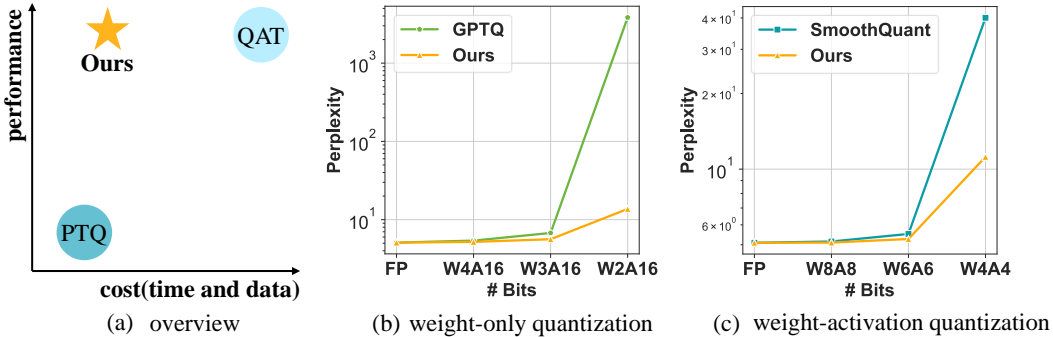


Figure 1: (a) provides a performance overview of the proposed OmniQuant, highlighting its ability to achieve quantization-aware training (QAT) performance with post-training quantization (PTQ) time and data efficiency. (b) and (c) showcase the perplexity (low is better) of quantized LLaMA-13B across different bit-widths on WikiText2.

quantization-aware training (QAT). Although QAT can lead to more competitive accuracy than PTQ, it is not practical due to the high training cost because the whole model is trained with the awareness of the quantization process. As a result, PTQ is commonly utilized in existing quantization methods on LLMs. For example, lots of PTQ methods (Frantar et al. (2022); Lin et al. (2023); Dettmers et al. (2023b); Lee et al. (2023)) reduce memory consumption by weight-only quantization which quantizes the weights while maintaining full-precision activation. To further reduce the computational overhead, another line of work (Xiao et al. (2023); Wei et al. (2022); Yuan et al. (2023); Wei et al. (2023)) employs weight-activation quantization which quantizes both weight and activation into low-bit values for the execution of low-bit matrix multiplication.

Existing quantization methods have demonstrated significant achievements in various scenarios, including W4A16 (*i.e.* 4-bit weight and 16-bit activation) weight-only quantization such as (Lin et al. (2023); Dettmers et al. (2023b); Lee et al. (2023)), as well as W8A8 weight-activation quantization (Wei et al. (2023)). However, they usually exhibit significant performance degradation when confronted with low-bit quantization, such as W2A16 and W4A4, as illustrated in Figure 1 (b & c). This performance shortfall in low-bit quantization can be attributed to the fact that these methods (Frantar et al. (2022); Lin et al. (2023); Wei et al. (2023)) primarily rely on handcrafted quantization parameters such as migration strength (Xiao et al. (2023)) and scaling parameters (Wei et al. (2023)), which often leads to lower performance. Although Quantization-Aware Training (QAT) (Liu et al. (2023a)) is effective in determining the optimal quantization configurations, it introduces substantial training overhead in both training and data efficiency. It is thus hard to quantize LLMs with QAT-based techniques efficiently such as LLMQAT (Liu et al. (2023a)). For instance, GPTQ (Frantar et al. (2022)), a PTQ approach, can complete the quantization of LLaMA-13B in an hour using 128 samples on a single A100 GPU, while LLM-QAT (Liu et al. (2023a)) requires 100k samples and hundreds of GPU hours. This leads us to a central question: *can we attain the performance of QAT, while maintaining the time and data efficiency of PTQ?*

This paper introduces a novel quantization technique, OmniQuant, which effectively addresses the above question. OmniQuant achieves state-of-the-art performance across various quantization scenarios, particularly in low-bit settings, while preserving the time and data efficiency of PTQ, as illustrated in Figure 1. Unlike Quantization-Aware Training (QAT) (Liu et al. (2023a)) which involves cumbersome weight optimization, OmniQuant freezes the original full-precision weight and only incorporates a few learnable quantization parameters. As shown in Figure 2, OmniQuant consists of two key components that incorporate different types of learnable quantization parameters, including Learnable Weight Clipping (LWC) and Learnable Equivalent Transformation (LET). Specifically, LWC modulates the extreme values of weights by optimizing the clipping threshold. In the meanwhile, LET tackles activation outliers by learning mathematically equivalent transformations in a transformer encoder.

Instead of jointly optimizing all parameters across the LLM, OmniQuant sequentially quantizes the parameters of one layer before moving on to the next under a block-wise quantization error

minimization framework. In this way, OmniQuant can be optimized efficiently using a simple Stochastic Gradient Descent (SGD) algorithm. Thanks to the differentiable optimization, LWC and LET can be seamlessly integrated into the quantization. We find that LWC can mitigate the difficulty in quantizing weights and LET further shifts the challenge of quantization from activations to weights, facilitating OmniQuant a versatile quantization framework for both weight-only and weight-activation quantization. Notably, OmniQuant introduces no extra computation or parameters for the quantized model because the clipping threshold in LWC and equivalent factors in LET can be fused into quantized weights.

As depicted in Figure 2, OmniQuant is easy to implement even with limited resources. Especially, taking the LLaMA-2 model family (7B-70B) as an example, all models can be quantized on a single A100-40G GPU utilizing only 128 training samples. The training time ranges from 1 to 16 hours, depending on the size of the quantized model, which ranges from 7B to 70B. Owing to the seamless integration of LWC and LET achieved by differentiable optimization, OmniQuant exhibits superior performance compared to prior PTQ-based methods in various quantization settings. For example, when LLaMA-13B is quantized into W2A16, OmniQuant achieves a perplexity of 13.21, while GPTQ incurs a significant increase in perplexity to 3832, as demonstrated in Figure 1. A similar performance advancement is also observed in the W4A4 quantization.

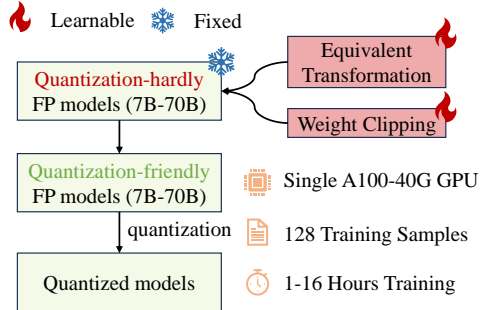


Figure 2: Characteristics of OmniQuant on LLaMA family.

The contributions of **OmniQuant** are summarized as follows. 1) We formulate a novel quantization pipeline for LLM, OmniQuant, which freezes original full-precision weights while incorporating a restrained set of learnable parameters. OmniQuant imbues quantization with gradient updates while preserving the time and data efficiency of PTQ methods. 2) OmniQuant consists of Learnable Weight Clipping (LWC) and Learnable Equivalent Transformation (LET). These strategies make full-precision weights and activations more amenable to quantization. 3) Through extensive experiments, we demonstrate that OmniQuant outperforms previous methods across a spectrum of quantization settings (W416, W3A16, W2A16, W6A6, W4A4), various model families (OPT, LLaMA, LLaMA-2, LLaMA-2-chat), and a range of model sizes (125M-70B). The computation speedup and memory reduction of OmniQuant are also demonstrated on real devices.

2 RELATED WORK

2.1 QUANTIZATION METHODS.

Quantization compresses neural networks by reducing bit-precision, facilitating decreased model size and enhanced inference speed. Presently, quantization methods fall into two primary categories: Quantization Aware Training (QAT) (Liu et al. (2023a)) and Post-training Quantization (PTQ) (Xiao et al. (2023); Frantar et al. (2022)). By simulating quantization during training and searching optimal quantization parameters to minimize accuracy degradation, QAT helps preserve model performance even under lower-precision settings. However, it is impractical to use QAT in the context of LLM due to its significant training expense. Some PTQ techniques, such as AdaRound (Nagel et al. (2020)) and BRECQ (Li et al. (2021)), employ gradient optimization and tune all weights to identify the optimal rounding operation in a data-efficient way. Nonetheless, adjusting all weights becomes time-consuming for models with billions of parameters. As a result, most extant quantization methods on LLMs (Xiao et al. (2023); Frantar et al. (2022); Dettmers et al. (2023b); Lee et al. (2023); Wei et al. (2023)) focus on training-free PTQ. However, the training-free method hinders the performance in the lower-bit scenario. In this work, we aim to incorporate gradient updates into LLM quantization like QAT while preserving the training time and data efficiency of PTQ.

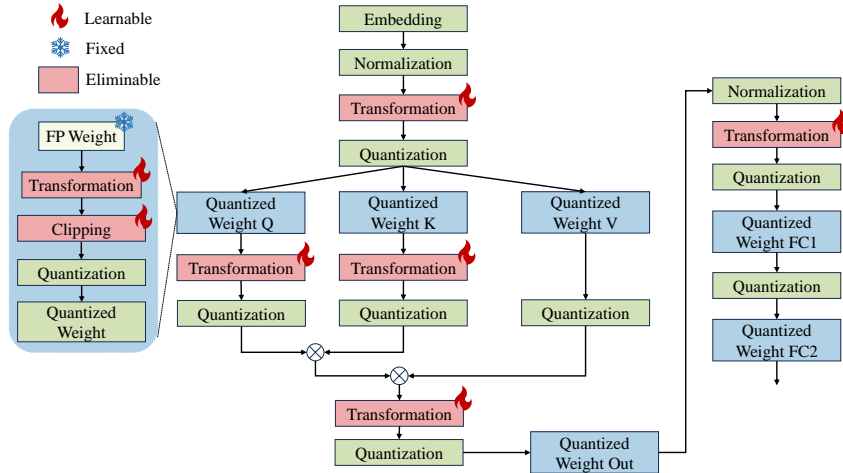


Figure 3: **Details of OmniQuant** in a transformer block. Note that the learnable equivalent transformation can be absorbed by the normalization layer and linear layer. The learnable clipping threshold applies only to float-point weight and thus can be discarded after quantization. Therefore, OmniQuant does not introduce any additional computation cost or parameters after quantization.

2.2 QUANTIZATION OF LLM.

Consider the quantized object, exiting LLM quantization can be classified into two fields: weight-only quantization (Frantar et al. (2022); Lin et al. (2023); Dettmers et al. (2023b); Lee et al. (2023); Chai et al. (2023); Dettmers et al. (2023a); Chee et al. (2023); Park et al. (2022)) and weight-activation quantization (Dettmers et al. (2022); Yao et al. (2022); Xiao et al. (2023); Wei et al. (2022; 2023); Yuan et al. (2023); Liu et al. (2023a)).

Weight-only quantization. Weight-only quantization exclusively converts weights into low-bit values. For example, GPTQ (Frantar et al. (2022)) achieves 3/4-bit quantization using block-wise reconstruction. SpQR (Dettmers et al. (2023b)), OWQ (Lee et al. (2023)), and AWQ (Lin et al. (2023)) observe that weights related to activations of higher magnitude play a pivotal role in the final performance. Therefore, SpQR and OWQ safeguard these vital weights using mixed-precision quantization. In contrast, AWQ protects them via channel-wise scaling, circumventing the hardware inefficiency linked to mixed-precision quantization. Both Qlora (Dettmers et al. (2023a)) and INT2.1 (Chee et al. (2023)) restore the capabilities of the quantized model through parameter-efficient fine-tuning. While our technique introduces additional learnable parameters, it differs fundamentally from Qlora and INT2.1. Specifically, Qlora and INT2.1 integrate learnable parameters post-quantization, whereas our approach aims to enhance the quantization process itself. Consequently, our proposed OmniQuant can be viewed as complementary to both Qlora and INT2.1.

Weight-activation quantization. Weight-activation quantization compresses both weights and activations into low-bit values. SmoothQuant (Xiao et al. (2023)), LLM.int8() (Dettmers et al. (2022)), Outlier Suppression (Wei et al. (2022)) accomplish W8A8 quantization by addressing outlier issues in activations. In particular, LLM.int8() employs mixed-precision decomposition, segregating outlier feature dimensions into a 16-bit matrix multiplication. Both Outlier Suppression and SmoothQuant adopt channel-wise scaling to curtail outlier magnitudes. Furthermore, Outlier Suppression+ (Wei et al. (2023)) integrates channel-wise shifting to further drive W6A6 quantization. Our approach also embraces channel-wise equivalent transformations. However, in contrast to heuristic designs (Xiao et al. (2023); Wei et al. (2022; 2023)), we utilize gradient optimization to determine the best solutions. We also extend equivalent transformations to attention mechanisms, not just confining them to linear layers, enhancing the quantization of the K/V cache. Recently, RPTQ (Yuan et al. (2023)) and LLM-QAT (Liu et al. (2023a)) pushed the quantization levels down to W4A4. RPTQ segments activations into multiple groups according to clustering, subsequently employing group-wise activation quantization. LLM-QAT conducts data-free QAT, leveraging outputs generated by the pre-trained model. In distinction from RPTQ and LLM-QAT, we achieve W4A4 through deployment-friendly per-token quantization and maintain the PTQ efficiency.

3 OMNIQUANT

Challenge of LLM quantization. Two main difficulties lie in quantizing an LLM. First, the activation is hard to quantize due to the existence of outlier channels. Considering that weight distribution is flat and uniform, SmoothQuant (Xiao et al. (2023)) and Outlier Suppression+ (Wei et al. (2023)) tackle this issue by migrating the quantization difficulty from activations to weights with a pre-defined migration strength. Second, the quantization error of weights also plays a pivotal role in the final performance due to the importance of weights corresponding to activations. SqQR (Dettmers et al. (2023b)) and OWQ (Lee et al. (2023)) propose to retain crucial weights in full-precision, while AWQ (Lin et al. (2023)) safeguards these weights using grid-searched channel-wise scaling. Although these methods have achieved certain success in compressing various LLMs, they often lead to suboptimal performance and fail to deal with extremely low-bit quantization due to the crude design of hand-crafted quantization parameters such as migration strength and scaling factors.

In this section, we introduce a differentiable quantization technique for LLM called **OmniQuant** where quantization parameters are learned with better flexibility. Towards this goal, OmniQuant is implemented with a block-wise quantization error minimization framework as presented in Sec.3.1. To tackle the aforementioned challenges of LLM quantization, we devise two novel strategies for additional learnable quantization parameters including a learnable weight clipping (LWC) to mitigate the difficulty in quantizing weights and a learnable equivalent transformation (LET) to further shift the challenge of quantization from activations to weights. We introduce LWC and LCT in Sec. 3.2 and Sec. 3.3, respectively.

3.1 BLOCK-WISE QUANTIZATION ERROR MINIMIZATION

Previous PTQ methods with gradient optimization, such as AdaRound (Nagel et al. (2020)), BRECQ (Li et al. (2021)) cannot be applied in models with billions of parameters because they are hard to optimize due to the huge solution space. Instead of turning the whole model, we propose a new optimization pipeline with block-wise quantization error minimization where the additional quantization parameters can be optimized in a differentiable manner. We formulate the optimization goal as follows.

$$\arg \min_{\Theta_1, \Theta_2} \|\mathcal{F}(\mathbf{W}, \mathbf{X}) - \mathcal{F}(Q_w(\mathbf{W}; \Theta_1, \Theta_2), Q_a(\mathbf{X}, \Theta_2))\|, \quad (1)$$

where \mathcal{F} represents the mapping function for a transformer block in the LLM, \mathbf{W} and \mathbf{X} are full-precision weight and activation, $Q_w(\cdot)$ and $Q_a(\cdot)$ represent weight and activation quantizer, respectively, Θ_1 and Θ_2 are quantization parameters in learnable weight clipping (LWC) and learnable equivalent transformation (LET), respectively. The Block-wise quantization in Eqn.(1) sequentially quantizes the parameters of one transformer block before moving on to the next.

Block-wise minimization in Eqn.(1) has two advantages. First, equipped with block-wise minimization in Eqn.(1), OmniQuant can optimize quantization parameters in LWC and LET jointly, making it capable enough to encompass both weight-only and weight-activation quantization. Second, block-wise minimization is easy to optimize with minimal resource requirements. OmniQuant only determines a few quantization parameters with optimality, which is easier than optimizing the whole weights in previous PTQ-based methods (Nagel et al. (2020); Li et al. (2021)). Empirically, we find that all models from the LLaMA-2 family (Touvron et al. (2023b)) can be quantized on a single A100-40G GPU utilizing only 128 training samples.

3.2 LEARNABLE WEIGHT CLIPPING

OmniQuant employs a module of learnable weight clipping (LWC) to reduce the difficulty of quantizing the weights in an LLM. Similar to previous methods with learnable clipping threshold (Esser et al. (2019); Liu et al. (2022); Choi et al. (2018)), LWC also determines the optimal dynamic range of the weights by optimizing a clipping threshold. However, we find that directly employing prior arts such as PACT (Choi et al. (2018)) and LSQ (Esser et al. (2019)) in quantization would produce unsatisfactory performance, as demonstrated in LLM-QAT (Liu et al. (2023a)). A similar result has been also observed in Table A3 in the Appendix.

Instead of directly learning a clipping threshold as did in previous methods (Esser et al. (2019); Choi et al. (2018)), LWC optimizes a clipping strength as formulated by

$$\mathbf{W}_q = \text{clamp}(\lfloor \frac{\mathbf{W}}{h} \rfloor + z, 0, 2^N - 1), \text{ where } h = \frac{\gamma \max(\mathbf{W}) - \beta \min(\mathbf{W})}{2^N - 1}, z = -\lfloor \frac{\beta \min(\mathbf{W})}{h} \rfloor \quad (2)$$

where $\lfloor \cdot \rfloor$ indicates round operation. N is the target bit number. \mathbf{W}_q and \mathbf{W} denote the quantized and full-precision weights, respectively. h is the normalization factor for weights and z is the zero-point value. The clamp operation constrains the value within the range of N -bit integer, specifically $[0, 2^N - 1]$. In Eqn.(2), $\gamma \in [0, 1]$ and $\beta \in [0, 1]$ are learnable clipping strengths for the upper and the lower bound of weights, respectively. We instantiate γ and β by the sigmoid function*. Hence, $\Theta_1 = \{\gamma, \beta\}$ in Eqn.(1).

Note that LWC degrades into a vanilla MinMax quantization scheme used in existing works (Xiao et al. (2023), Frantar et al. (2022)) when $\gamma = 1$ and $\beta = 1$. By inheriting the benefits of MinMax quantization, LWC only needs to adjust the clipping strengths to determine an optimal clipping strength, which would reduce the optimization difficulty. Clipped by an optimal threshold, the original weights would be easy to quantize. As indicated by the experiments in Table 1, our proposed learnable weight clipping method significantly outperforms previous weight-only quantization techniques (Frantar et al. (2022); Lin et al. (2023)).

3.3 LEARNABLE EQUIVALENT TRANSFORMATION

Other than LWC which enables quantization-friendly weights by optimizing the clipping threshold, we further reduce the difficulty of weight-activation quantization by a learnable equivalent transformation (LET). Considering that outliers in the activation map are systematic and unique to specific channels, previous methods such as SmoothQuant (Xiao et al. (2023)) migrate the difficulty of quantization from activations to weights with a mathematically equivalent transformation. However, they hand-craft the equivalent parameters, leading to suboptimal results.

Thanks to the inclusion of block-wise quantization error minimization, our LET can determine the optimal equivalent parameters in a differentiable way. Inspired by SmoothQuant (Xiao et al. (2023)) and Outlier Suppression+ (Wei et al. (2023)), we adopt channel-wise scaling and channel-wise shifting to manipulate the activation distribution, providing an effective solution for the outlier issue. Specifically, we investigate the equivalent transformation across both the linear layer and attention operation, as illustrated in Figure3.

Linear layer. The linear layer takes an input token sequence $\mathbf{X} \in \mathbb{R}^{T \times C_{in}}$ where T is the token length and is the multiplication of the weight matrix $\mathbf{W} \in \mathbb{R}^{C_{in} \times C_{out}}$ and bias vector $\mathbf{B} \in \mathbb{R}^{1 \times C_{out}}$. A mathematically equivalent linear layer is expressed as:

$$\mathbf{Y} = \mathbf{X}\mathbf{W} + \mathbf{B} = \underbrace{[(\mathbf{X} - \delta) \oslash \mathbf{s}]}_{\tilde{\mathbf{X}}} \cdot \underbrace{[\mathbf{s} \odot \mathbf{W}]}_{\tilde{\mathbf{W}}} + \underbrace{[\mathbf{B} + \delta \mathbf{W}]}_{\tilde{\mathbf{B}}} \quad (3)$$

where \mathbf{Y} represents the output, $\mathbf{s} \in \mathbb{R}^{1 \times C_{in}}$ and $\delta \in \mathbb{R}^{1 \times C_{in}}$ are channel-wise scaling and shifting parameters, respectively, $\tilde{\mathbf{X}}$, $\tilde{\mathbf{W}}$ and $\tilde{\mathbf{B}}$ are equivalent activation, weight and bias, respectively, ' \oslash ' and ' \odot ' are elementwise division and multiplication. By Eqn.(3), the activations are transformed to be quantization-friendly at a cost of increased quantization difficulty in weights. In this sense, LWC in Sec. 3.2 can improve the performance of weight-activation quantization achieved by LET because it renders weights quantization-friendly. Finally, we perform quantization on transformed activations and weights, as given by

$$\mathbf{Y} = Q_a(\tilde{\mathbf{X}})Q_w(\tilde{\mathbf{W}}) + \tilde{\mathbf{B}}, \quad (4)$$

where Q_a is the vanilla MinMax quantizer and Q_w is the MinMax quantizer with learnable weight clipping (i.e. our LWC).

Note that the scaling and shifting parameters in $\tilde{\mathbf{X}}$ can be absorbed into the previous normalization or linear layer and the scaling factors in $\tilde{\mathbf{W}}$ can be fused into the original linear weight \mathbf{W} . Therefore, the equivalent transformation in Eqn.(3) can effectively reduce quantization errors

*Sigmoid(t) = $1/(1 + \exp^{-t})$

without introducing additional parameters or costs. We employ this equivalent transformation in all linear layers of the LLM except for the second linear layer of FFN as shown in Figure 3. This may be because the high sparsity of features after the non-linear layer (Liu et al. (2023b)) leads to unstable gradients when applying learnable equivalent transformations.

Attention operation. Beyond the linear layer, the attention operation also accounts for a significant proportion of the computation. Additionally, the auto-regressive pattern of LLM necessitates storing the key-value(KV) cache for each token, which results in substantial memory demands for long sequences. Therefore, we also quantize $\mathbf{Q}/\mathbf{K}/\mathbf{V}$ matrixes into low-bit in the weight-activation quantization setting. Specifically, the learnable equivalent transform of the self-attention affinity matrix can be written as:

$$\mathbf{P} = \text{Softmax}(\mathbf{Q}\mathbf{K}^T) = \text{Softmax}(\underbrace{(\mathbf{Q} \oslash s_a)}_{\tilde{\mathbf{Q}}}\underbrace{(s_a \odot \mathbf{K}^T)}_{\tilde{\mathbf{K}}^T}). \quad (5)$$

where $s_a \in \mathbb{R}^{1 \times C_{out}}$ is the scaling factor in the affinity matrix. Similar to Eqn.(4), the quantized affinity matrix calculation is expressed as $\mathbf{P} = \text{Softmax}(Q_a(\tilde{\mathbf{Q}})Q_a(\tilde{\mathbf{K}}^T))$. Here we also use Min-Max quantization scheme as Q_a to quantize $\tilde{\mathbf{Q}}/\tilde{\mathbf{K}}$ matrixes. From Eqn.(4) and Eqn.(5) we know that $\Theta_2 = \{\delta, s, s_a\}$ in Eqn.(1).

The channel-wise scaling factors in $\tilde{\mathbf{Q}}$ and $\tilde{\mathbf{K}}$, as seen in Eq.(5), can be absorbed into linear weights of the query and key projection, respectively. It is worth mentioning that the explicit transformation of \mathbf{V} is omitted as its distribution has already been channel-wise altered by the inverse transformation associated with the output projection linear layer.

4 EXPERIMENTS

4.1 SETTINGS

Quantization. We conduct experiments in comprehensive quantization settings, encompassing both weight-only quantization and weight-activation quantization. In weight-only quantization, we explore INT4/INT3/INT2, with per-channel weight quantization as the default setting, unless stated otherwise. Additionally, we investigate group-wise weight quantization, represented as ‘g’. For example, W3A16g128 denotes weight-only quantization with a group size of 128. For weight-activation quantization, we explore INT6/INT4, utilizing per-channel weight quantization and per-token activation quantization (Dettmers et al. (2022)) as the default. Note that we quantized all intermediate activation into low-bit, except the SoftMax output, which is retained at full precision. This is attributed to the fact that SoftMax output follows a long-tail distribution, rendering it unsuitable for the uniform quantization studied in this study.

Training The channel-wise scaling factor β is initialized with SmoothQuant (Xiao et al. (2023)), and the channel-wise shifting factor is initialized using Outlier Suppression+ (Wei et al. (2023)). To optimize the learnable parameters, we utilize the AdamW optimizer with zero weight decay. The learning rate for learnable weight clipping and learnable equivalent transformation is set as $5e - 3$ and $1e - 2$, respectively. We employ a calibration dataset consisting of 128 randomly selected 2048-token segments from WikiText2 (Merity et al. (2016)). The entire training process is facilitated on a single Nvidia A100 GPU, utilizing a batch size of 1 over 20 epochs, except for W2A16 quantization that leverages 40 epochs. For weight-activation quantization, we activate both learnable weight clipping and learnable equivalent transformation. Conversely, for weight-only quantization, both mechanisms are activated for OPT, but only learnable weight clipping is utilized for LLaMA. This is attributable to the fact that the learnable equivalent transformation yields negligible benefits for LLaMA’s weight-only quantization, as demonstrated in Table 4.

Models. We firstly evaluate our method on OPT(125M-66B) (Zhang et al. (2022)), LLaMA(7B-65B) (Touvron et al. (2023a)), and LLaMA-2(7B-70B) (Touvron et al. (2023b)) families. Furthermore, we extend our benchmarking to the instruction-tuned model, LLaMA-2-chat (7B-70B) (Touvron et al. (2023b)), to demonstrate the generalizability of our approach.

Evaluation. Following the previous work (Lin et al. (2023); Frantar et al. (2022); Dettmers & Zettlemoyer (2023); Yuan et al. (2023); Liu et al. (2023a)), we evaluate quantized models by reporting the perplexity of language generation experiments, specifically on WikiText2 (Merity et al.

Table 1: **Weight-only quantization Results of LLaMA-1 and LLaMA-2 Models.** We report WikiText2 perplexity in this table, C4 perplexity can be found in Table A8 in Appendix.

LLaMA1&2 / PPL↓		1-7B	1-13B	1-30B	1-65B	2-7B	2-13B	2-70B
FP16	-	5.68	5.09	4.10	3.53	5.47	4.88	3.31
W2A16	RTN	1.1e5	6.8e4	2.4e4	2.2e4	3.8e4	5.6e4	2.0e4
	GPTQ	2.1e3	5.5e3	499.75	55.91	7.7e3	2.1e3	77.95
	OmniQuant	15.47	13.21	8.71	7.58	37.37	17.21	7.81
W2A16 g128	RTN	1.9e3	781.20	68.04	15.08	4.2e3	122.08	27.27
	GPTQ	44.01	15.60	10.92	9.51	36.77	28.14	NAN
	OmniQuant	10.53	8.37	7.77	6.35	12.84	9.15	7.82
W2A16 g64	RTN	188.32	101.87	19.20	9.39	431.97	26.22	10.31
	GPTQ	22.10	10.06	8.54	8.31	20.85	22.44	NAN
	OmniQuant	9.41	7.62	7.14	6.01	10.56	8.14	6.88
W3A16	RTN	25.73	11.39	14.95	10.68	539.48	10.68	7.52
	GPTQ	8.06	6.76	5.84	5.06	8.37	6.44	4.82
	OmniQuant	6.49	5.68	4.74	4.04	6.58	5.58	3.92
W3A16 g128	RTN	7.01	5.88	4.87	4.24	6.66	5.51	3.97
	GPTQ	6.55	5.62	4.80	4.17	6.29	5.42	3.85
	OmniQuant	6.15	5.44	4.56	3.94	6.03	5.28	3.78
W4A16	RTN	6.43	5.55	4.57	3.87	6.11	5.20	3.67
	GPTQ	6.13	5.40	4.48	3.83	5.83	5.13	3.58
	OmniQuant	5.86	5.21	4.25	3.71	5.74	5.02	3.47
W4A16 g128	RTN	5.96	5.25	4.23	3.67	5.72	4.98	3.46
	GPTQ	5.85	5.20	4.23	3.65	5.61	4.98	3.42
	OmniQuant	5.77	5.17	4.19	3.62	5.58	4.95	3.40

(2016)), PTB (Marcus et al. (1994)), C4 (Raffel et al. (2020)). Note that perplexity serves as an indicator of the generative performance of models and has a high coefficient with zero-shot performance (Dettmers & Zettlemoyer (2023)). Moreover, accuracy is evaluated in zero-shot tasks including PIQA (Bisk et al. (2020)), ARC (Clark et al. (2018)), BoolQ (Clark et al. (2019)), and HellaSwag (Clark et al. (2018)). We adhere to the GPTQ (Frantar et al. (2022)) settings for language generation experiments, and implement the lm-eval-harness (Gao et al. (2021)) for the execution of all zero-shot tasks.

Baselines. For weight-only quantization, we draw comparisons with vanilla round-to-nearest quantization (RTN), reconstruction method GPTQ (Frantar et al. (2022)), and group-wise quantization method AWQ (Lin et al. (2023)). For weight-activation quantization, we compare our method with smoothquant (Xiao et al. (2023)), RPTQ (Yuan et al. (2023)), and the recent QAT method LLM-QAT (Liu et al. (2023a)). We reproduce SmoothQuant with per-channel weight quantization and per-token activation quantization for fair comparisons. It should be noted that RPTQ (Yuan et al. (2023)) retains the output activation of layer normalization and softmax at 8-bit precision. To ensure a fair comparison, we also replicate it with our setup, quantizing all activations into low-bit except keeping the softmax output at full precision, which we denote as RPTQ*.

4.2 WEIGHT-ONLY QUANTIZATION RESULTS

The results of the LLaMA family can be found in Table 1, while the results for OPT are presented in the Sec. A6 of Appendix. As illustrated by the tables, OmniQuant consistently outperforms the prior LLM weight-only quantization method across various LLM families (OPT, LLaMA-1, LLaMA-2) and diverse quantization configurations, including W2A16, W2A16g128, W2A16g64, W3A16, W3A16g128, W4A16, and W4A16g128. These findings suggest OmniQuant’s versatility, being adaptable to a multitude of quantization configurations. For instance, while AWQ (Lin et al. (2023)) is particularly effective with group-wise quantization, OmniQuant demonstrates superior

Table 2: **Weight-activation quantization results of LLaMA Models.** This table reports the accuracy of 6 zero-shot tasks. Perplexity results can be found in Table A12 & A13 at Appendix.

LLaMA / Acc \uparrow	#Bits	Method	PIQA	ARC-e	Arc-c	BoolQ	HellaSwag	Winogrande	Avg.
LLaMA-1-7B	FP16	-	77.47	52.48	41.46	73.08	73.00	67.07	64.09
	W6A6	SmoothQuant	76.75	51.64	39.88	71.75	71.67	65.03	62.81
	W6A6	OmniQuant	77.09	51.89	40.87	72.53	71.61	65.03	63.17
	W4A4	SmoothQuant	49.80	30.40	25.80	49.10	27.40	48.00	38.41
	W4A4	LLM-QAT	51.50	27.90	23.90	61.30	31.10	51.90	41.27
	W4A4	LLM-QAT+SQ	55.90	35.50	26.40	62.40	47.80	50.60	46.43
	W4A4	OmniQuant	66.15	45.20	31.14	63.51	56.44	53.43	52.65
LLaMA-1-13B	FP16	-	79.10	59.89	44.45	68.01	76.21	70.31	66.33
	W6A6	SmoothQuant	77.91	56.60	42.40	64.95	75.36	69.36	64.43
	W6A6	OmniQuant	78.40	57.28	42.91	67.00	75.82	68.27	64.95
	W4A4	SmoothQuant	61.04	39.18	30.80	61.80	52.29	51.06	49.36
	W4A4	OmniQuant	69.69	47.39	33.10	62.84	58.96	55.80	54.37
LLaMA-1-30B	FP16	-	80.08	58.92	45.47	68.44	79.21	72.53	67.44
	W6A6	SmoothQuant	77.14	57.61	42.91	65.56	78.07	69.92	65.20
	W6A6	OmniQuant	79.81	58.79	45.22	68.38	78.95	72.21	67.23
	W4A4	SmoothQuant	58.65	35.53	27.73	60.42	35.56	48.06	44.83
	W4A4	OmniQuant	71.21	49.45	34.47	65.33	64.65	59.19	56.63
LLaMA-1-65B	FP16	-	80.79	58.71	46.24	82.29	80.72	77.50	71.04
	W6A6	SmoothQuant	80.25	57.92	45.50	80.22	80.18	74.76	69.80
	W6A6	OmniQuant	81.01	58.12	46.33	80.64	79.91	75.69	70.28
	W4A4	SmoothQuant	64.47	40.44	29.82	59.38	39.90	52.24	47.71
	W4A4	OmniQuant	71.81	48.02	35.92	73.27	66.81	59.51	59.22

performance across both channel-wise and group-wise quantization. Furthermore, the performance benefits of OmniQuant become more pronounced as the quantization bit size decreases.

Interestingly, even with learnable weight clipping applied to LLaMA alone, OmniQuant can achieve a significant performance improvement compared to previous methods, thus highlighting the effectiveness of our proposed learnable weight clipping. In addition, all of OmniQuant’s learnable parameters can be eliminated, making it compatible with existing weight-only quantization kernels for deployment. For instance, Table 3 demonstrates that W4A16g128 and W2A16g128 can achieve nearly $2\times$ inference speedup compared to full-precision (16-bit).

4.3 WEIGHT-ACTIVATION QUANTIZATION RESULTS

In weight-activation quantization, our main focus lies on W6A6 and W4A4 quantization. We exclude W8A8 quantization as SmoothQuant can nearly achieve lossless W8A8 quantized models when compared with full-precision counterparts. The results of the LLaMA family can be found in Table 2, while the results for OPT are presented in Table A14 of Appendix. Table 2 illustrates the zero-shot task accuracy of LLaMA weight-activation quantization. Notably, OmniQuant markedly enhances the average accuracy by +4.99% +11.80% across various models at W4A4 quantization. Remarkably, in the LLaMA-7B, OmniQuant even surpasses the recent QAT method, LLM-QAT (Liu et al. (2023a)), by an impressive margin of +6.22%. This improvement demonstrates the efficacy of incorporating additional learnable parameters, which proves to be more beneficial than the global weight tuning utilized by QAT. Considering that W4A4 and W6A6 quantization methods lack out-of-the-box hardware support, this study does not incorporate hardware implementation.

4.4 QUANTIZATION OF INSTRUCTION-TUNED MODELS

To demonstrate the generalization ability of the proposed method, we benchmark the quantization method on LLaMA-2-chat (Touvron et al. (2023b))). This model is instruction-tuned and suitable for chatbot applications. We adopt the GPT-4 evaluation protocol (Chiang et al. (2023)) to assess the performance of the quantized method using the Vicuna (Chiang et al. (2023)) benchmark, which comprises 80 sampled questions. To eliminate position bias (Zheng et al. (2023)), we compared each pair in both orders (a v.s. b and b v.s. a), resulting in 160 trials for each comparison pair. As depicted in Figure 4, we compare RTN, AWQ (Lin et al. (2023)), and our proposed OmniQuant. In

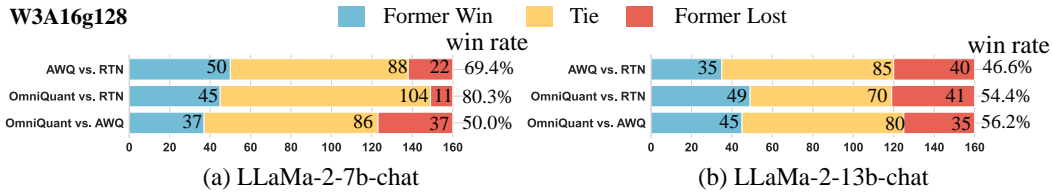


Figure 4: Comparing W3A16g128 quantization among RTN, AWQ (Lin et al. (2023)), and proposed OmniQuant under GPT-4 evaluation protocol (Chiang et al. (2023)). Win rates are calculated without considering tie samples. A higher win rate indicates the better performance of the former of vs. pairs.

the LLaMA-2-7b-chat results, OmniQuant and AWQ are evenly matched with a 50% win rate, but OmniQuant outperforms RTN more (80.3% v.s. 69.4%). For LLaMA-2-13b-chat, AWQ underperforms relative to RTN. However, OmniQuant consistently enhances the performance of quantization models.

4.5 ACCELERATION ON REAL DEVICE

MLC-LLM[†] offers a universal deployment solution suitable for various language models across a wide range of hardware backends, encompassing iPhones, Android phones, and GPUs from NVIDIA, AMD, and Intel. Notably, MLC-LLM emerges as the optimal solution for deploying quantized models on CUDA. A notable advantage of OmniQuant is that it does not introduce additional operations for quantized models. Consequently, MLC-LLM can natively execute the quantized models developed using OmniQuant. Table 3 delineates the memory requirements and inference speeds of the LLaMA family on a single NVIDIA A100-80G. ‘Weights memory’ characterizes the storage utilized by quantized weights, while ‘Running memory’ signifies the memory needed for practical inference. The latter is notably greater due to the need to retain certain intermediate activations. Our evaluation metric for inference speed was the generation of 512 tokens from scratch. It is evident that quantized models drastically curtail memory usage compared to the full-precision (16-bit) counterparts. Further, models W4A16g128 and W2A16g128 display nearly a 2× enhancement in inference speed.

Table 3: Deployment of weight-only quantization through MLC-LLM. We report the memory size of quantized weights (denoted as ‘WM’) and the running memory (denoted as ‘RM’) and speed in NVIDIA A100-80G.

LLaMA	7B			13B			30B			65B		
	WM	RM	token/s	WM	RM	token/s	WM	RM	token/s	WM	RM	token/s
FP	12.6G	14.4G	69.2	24.3G	27.1G	52.5	60.6G	66.1G	23.9	OOM	-	-
W4A16g128	3.8G	5.7G	134.2	7.0G	10.0G	91.3	16.7G	21.7G	43.6	33.0G	41.0G	24.3
W3A16g128	3.2G	5.1G	83.4	5.8G	8.7G	57.6	13.7G	18.7G	29.0	27.0G	35.1G	15.2
W2A16g128	2.2G	4.1G	83.9	4.0G	7.5G	92.6	9.2G	14.1G	36.7	18.0G	25.6G	24.8

Table 4: **Ablation studies.** WikiText2 perplexity1 is reported in this table. ‘-’ indicates remove the corresponding module from the overall proposed methods.

Method	PPL↓	LLaMA-13B		OPT-13B	
		W4A4	W3A16	W4A4	W3A16
	LWC+LET	10.87	5.65	11.65	10.87
components	-LWC	20.75	7.65	15.23	12.98
	-LET	5.4e3	5.68	7.8e3	11.29
	-LWC-LET	1.8e3	10.68	7.8e5	4.6e3

[†]<https://github.com/mlc-ai/mlc-llm>

4.6 ABLATION STUDIES

In this section, we evaluate the performance contributions of LWC and LET. Further ablation studies, encompassing the design of LET, training duration, and calibration datasets, can be found in Appendix Sec A5. As demonstrated in Table 4, the baseline model activates both LWC and LET, labeled as 'LWC+LET'. Subsequently, the unique contributions of LWC and LET to overall performance are assessed by sequentially deactivating each. Unsurprisingly, each component has a positive impact on final performance. However, LET emerges as particularly critical in weight-activation quantization. When deactivated for W4A4, the model experiences a dramatic surge in perplexity to e^3 . This significant increase is attributed to the challenge posed by outliers in activation quantization, a problem effectively ameliorated by the implementation of LET. In the case of weight-only quantization, the implementation of LET substantially improves the performance of OPT, while only providing marginal improvement for LLaMA. This variation can be attributed to the minimal presence of outliers in LLaMA's weights. For instance, during naive W3A16 quantization (-LWC-LET), LLaMA's performance reaches a perplexity of 10.68, whereas OPT's perplexity dramatically escalates to $4.6e^3$. Hence, for weight-only quantization, LET is deactivated for LLaMA due to its negligible benefit.

5 CONCLUSION

In this study, we introduce OmniQuant, an innovative method designed to propel both weight-only quantization and weight-activation quantization into low-bit formats. The foundational insight of OmniQuant involves freezing the original full-precision weights while introducing additional learnable parameters. Specifically, OmniQuant leverages learnable weight clipping and learnable equivalent transformation to render weight and activation more compatible with quantization. Despite integrating gradient updates, OmniQuant conserves training time and data efficiency on par with prevalent PTQ methods. It surpasses existing techniques in language generation and zero-shot tasks and is viable for application in instruction-tuned LLMs. Additionally, OmniQuant demonstrates hardware efficiency as all additional learnable parameters can be absorbed, ensuring its compatibility with existing kernels.

ACKNOWLEDGMENTS

We thank Wentao Liu from SenseTime for his valuable insights and discussions regarding LLM deployment. We also acknowledge Siyuan Feng from Apache TVM for assisting in the successful deployment of our OmniQuant in the MLC LLM project.

REFERENCES

- Yonatan Bisk, Rowan Zellers, Jianfeng Gao, Yejin Choi, et al. Piqa: Reasoning about physical commonsense in natural language. In *Proceedings of the AAAI conference on artificial intelligence*, volume 34, pp. 7432–7439, 2020.
- Tom Brown, Benjamin Mann, Nick Ryder, Melanie Subbiah, Jared D Kaplan, Prafulla Dhariwal, Arvind Neelakantan, Pranav Shyam, Girish Sastry, Amanda Askell, et al. Language models are few-shot learners. *Advances in neural information processing systems*, 33:1877–1901, 2020.
- Sébastien Bubeck, Varun Chandrasekaran, Ronen Eldan, Johannes Gehrke, Eric Horvitz, Ece Kamar, Peter Lee, Yin Tat Lee, Yuanzhi Li, Scott Lundberg, et al. Sparks of artificial general intelligence: Early experiments with gpt-4. *arXiv preprint arXiv:2303.12712*, 2023.
- Yuji Chai, John Gkountouras, Glenn G Ko, David Brooks, and Gu-Yeon Wei. Int2. 1: Towards fine-tunable quantized large language models with error correction through low-rank adaptation. *arXiv preprint arXiv:2306.08162*, 2023.
- Jerry Chee, Yaohui Cai, Volodymyr Kuleshov, and Christopher De Sa. Quip: 2-bit quantization of large language models with guarantees. *arXiv preprint arXiv:2307.13304*, 2023.
- Wei-Lin Chiang, Zhuohan Li, Zi Lin, Ying Sheng, Zhanghao Wu, Hao Zhang, Lianmin Zheng, Siyuan Zhuang, Yonghao Zhuang, Joseph E. Gonzalez, Ion Stoica, and Eric P. Xing. Vicuna: An

- open-source chatbot impressing gpt-4 with 90%* chatgpt quality, March 2023. URL <https://lmsys.org/blog/2023-03-30-vicuna/>.
- Jungwook Choi, Zhuo Wang, Swagath Venkataramani, Pierce I-Jen Chuang, Vijayalakshmi Srivivasan, and Kailash Gopalakrishnan. Pact: Parameterized clipping activation for quantized neural networks. *arXiv preprint arXiv:1805.06085*, 2018.
- Christopher Clark, Kenton Lee, Ming-Wei Chang, Tom Kwiatkowski, Michael Collins, and Kristina Toutanova. Boolq: Exploring the surprising difficulty of natural yes/no questions. *arXiv preprint arXiv:1905.10044*, 2019.
- Peter Clark, Isaac Cowhey, Oren Etzioni, Tushar Khot, Ashish Sabharwal, Carissa Schoenick, and Oyvind Tafjord. Think you have solved question answering? try arc, the ai2 reasoning challenge. *arXiv preprint arXiv:1803.05457*, 2018.
- Tim Dettmers and Luke Zettlemoyer. The case for 4-bit precision: k-bit inference scaling laws. In *International Conference on Machine Learning*, pp. 7750–7774. PMLR, 2023.
- Tim Dettmers, Mike Lewis, Younes Belkada, and Luke Zettlemoyer. Llm.int8(): 8-bit matrix multiplication for transformers at scale. *arXiv preprint arXiv:2208.07339*, 2022.
- Tim Dettmers, Artidoro Pagnoni, Ari Holtzman, and Luke Zettlemoyer. Qlora: Efficient finetuning of quantized llms. *arXiv preprint arXiv:2305.14314*, 2023a.
- Tim Dettmers, Ruslan Svirschevski, Vage Egiazarian, Denis Kuznedelev, Elias Frantar, Saleh Ashkboos, Alexander Borzunov, Torsten Hoefler, and Dan Alistarh. Spqr: A sparse-quantized representation for near-lossless llm weight compression. *arXiv preprint arXiv:2306.03078*, 2023b.
- Steven K Esser, Jeffrey L McKinstry, Deepika Bablani, Rathinakumar Appuswamy, and Dharmendra S Modha. Learned step size quantization. *arXiv preprint arXiv:1902.08153*, 2019.
- Elias Frantar, Saleh Ashkboos, Torsten Hoefler, and Dan Alistarh. Gptq: Accurate post-training quantization for generative pre-trained transformers. *arXiv preprint arXiv:2210.17323*, 2022.
- Leo Gao, Stella Biderman, Sid Black, Laurence Golding, Travis Hoppe, Charles Foster, Jason Phang, Horace He, Anish Thite, Noa Nabeshima, et al. The pile: An 800gb dataset of diverse text for language modeling. *arXiv preprint arXiv:2101.00027*, 2020.
- Leo Gao, Jonathan Tow, Stella Biderman, Sid Black, Anthony DiPofi, Charles Foster, Laurence Golding, Jeffrey Hsu, Kyle McDonell, Niklas Muennighoff, et al. A framework for few-shot language model evaluation. *Version v0. 0.1. Sept*, 2021.
- Dan Hendrycks, Collin Burns, Steven Basart, Andy Zou, Mantas Mazeika, Dawn Song, and Jacob Steinhardt. Measuring massive multitask language understanding. *arXiv preprint arXiv:2009.03300*, 2020.
- Changhun Lee, Jungyu Jin, Taesu Kim, Hyungjun Kim, and Eunhyeok Park. Owq: Lessons learned from activation outliers for weight quantization in large language models. *arXiv preprint arXiv:2306.02272*, 2023.
- Yuhang Li, Ruihao Gong, Xu Tan, Yang Yang, Peng Hu, Qi Zhang, Fengwei Yu, Wei Wang, and Shi Gu. Brecq: Pushing the limit of post-training quantization by block reconstruction. *arXiv preprint arXiv:2102.05426*, 2021.
- Ji Lin, Jiaming Tang, Haotian Tang, Shang Yang, Xingyu Dang, and Song Han. Awq: Activation-aware weight quantization for llm compression and acceleration. *arXiv preprint arXiv:2306.00978*, 2023.
- Zechun Liu, Kwang-Ting Cheng, Dong Huang, Eric P Xing, and Zhiqiang Shen. Nonuniform-to-uniform quantization: Towards accurate quantization via generalized straight-through estimation. In *Proceedings of the IEEE/CVF Conference on Computer Vision and Pattern Recognition*, pp. 4942–4952, 2022.

- Zechun Liu, Barlas Oguz, Changsheng Zhao, Ernie Chang, Pierre Stock, Yashar Mehdad, Yangyang Shi, Raghuraman Krishnamoorthi, and Vikas Chandra. Llm-qat: Data-free quantization aware training for large language models. *arXiv preprint arXiv:2305.17888*, 2023a.
- Zichang Liu, Jue Wang, Tri Dao, Tianyi Zhou, Binhang Yuan, Zhao Song, Anshumali Shrivastava, Ce Zhang, Yuandong Tian, Christopher Re, et al. Deja vu: Contextual sparsity for efficient llms at inference time. In *International Conference on Machine Learning*, pp. 22137–22176. PMLR, 2023b.
- Mitch Marcus, Grace Kim, Mary Ann Marcinkiewicz, Robert MacIntyre, Ann Bies, Mark Ferguson, Karen Katz, and Britta Schasberger. The penn treebank: Annotating predicate argument structure. In *Human Language Technology: Proceedings of a Workshop held at Plainsboro, New Jersey, March 8-11, 1994*, 1994.
- Stephen Merity, Caiming Xiong, James Bradbury, and Richard Socher. Pointer sentinel mixture models. *arXiv preprint arXiv:1609.07843*, 2016.
- Yao Mu, Qinglong Zhang, Mengkang Hu, Wenhai Wang, Mingyu Ding, Jun Jin, Bin Wang, Jifeng Dai, Yu Qiao, and Ping Luo. Embodiedgpt: Vision-language pre-training via embodied chain of thought. *arXiv preprint arXiv:2305.15021*, 2023.
- Markus Nagel, Rana Ali Amjad, Mart Van Baalen, Christos Louizos, and Tijmen Blankevoort. Up or down? adaptive rounding for post-training quantization. In *International Conference on Machine Learning*, pp. 7197–7206. PMLR, 2020.
- Gunho Park, Baeseong Park, Se Jung Kwon, Byeongwook Kim, Youngjoo Lee, and Dongsoo Lee. nuqmm: Quantized matmul for efficient inference of large-scale generative language models. *arXiv preprint arXiv:2206.09557*, 2022.
- Colin Raffel, Noam Shazeer, Adam Roberts, Katherine Lee, Sharan Narang, Michael Matena, Yanqi Zhou, Wei Li, and Peter J Liu. Exploring the limits of transfer learning with a unified text-to-text transformer. *The Journal of Machine Learning Research*, 21(1):5485–5551, 2020.
- Hugo Touvron, Thibaut Lavril, Gautier Izacard, Xavier Martinet, Marie-Anne Lachaux, Timothée Lacroix, Baptiste Rozière, Naman Goyal, Eric Hambro, Faisal Azhar, et al. Llama: Open and efficient foundation language models. *arXiv preprint arXiv:2302.13971*, 2023a.
- Hugo Touvron, Louis Martin, Kevin Stone, Peter Albert, Amjad Almahairi, Yasmine Babaei, Nikolay Bashlykov, Soumya Batra, Prajjwal Bhargava, Shruti Bhosale, et al. Llama 2: Open foundation and fine-tuned chat models. *arXiv preprint arXiv:2307.09288*, 2023b.
- Xiuying Wei, Yunchen Zhang, Xiangguo Zhang, Ruihao Gong, Shanghang Zhang, Qi Zhang, Fengwei Yu, and Xianglong Liu. Outlier suppression: Pushing the limit of low-bit transformer language models. *Advances in Neural Information Processing Systems*, 35:17402–17414, 2022.
- Xiuying Wei, Yunchen Zhang, Yuhang Li, Xiangguo Zhang, Ruihao Gong, Jinyang Guo, and Xianglong Liu. Outlier suppression+: Accurate quantization of large language models by equivalent and optimal shifting and scaling. *arXiv preprint arXiv:2304.09145*, 2023.
- Guangxuan Xiao, Ji Lin, Mickael Seznec, Hao Wu, Julien Demouth, and Song Han. Smoothquant: Accurate and efficient post-training quantization for large language models. In *International Conference on Machine Learning*, pp. 38087–38099. PMLR, 2023.
- Peng Xu, Wenqi Shao, Kaipeng Zhang, Peng Gao, Shuo Liu, Meng Lei, Fanqing Meng, Siyuan Huang, Yu Qiao, and Ping Luo. Lvlm-ehub: A comprehensive evaluation benchmark for large vision-language models. *arXiv preprint arXiv:2306.09265*, 2023.
- Zhewei Yao, Reza Yazdani Aminabadi, Minjia Zhang, Xiaoxia Wu, Conglong Li, and Yuxiong He. Zeroquant: Efficient and affordable post-training quantization for large-scale transformers. *Advances in Neural Information Processing Systems*, 35:27168–27183, 2022.
- Zhihang Yuan, Lin Niu, Jiawei Liu, Wenyu Liu, Xinggang Wang, Yuzhang Shang, Guangyu Sun, Qiang Wu, Jiaying Wu, and Bingzhe Wu. Rptq: Reorder-based post-training quantization for large language models. *arXiv preprint arXiv:2304.01089*, 2023.

Rowan Zellers, Ari Holtzman, Yonatan Bisk, Ali Farhadi, and Yejin Choi. Hellaswag: Can a machine really finish your sentence? *arXiv preprint arXiv:1905.07830*, 2019.

Susan Zhang, Stephen Roller, Naman Goyal, Mikel Artetxe, Moya Chen, Shuohui Chen, Christopher Dewan, Mona Diab, Xian Li, Xi Victoria Lin, et al. Opt: Open pre-trained transformer language models. *arXiv preprint arXiv:2205.01068*, 2022.

Yiyuan Zhang, Kaixiong Gong, Kaipeng Zhang, Hongsheng Li, Yu Qiao, Wanli Ouyang, and Xiangyu Yue. Meta-transformer: A unified framework for multimodal learning. *arXiv preprint arXiv:2307.10802*, 2023.

Lianmin Zheng, Wei-Lin Chiang, Ying Sheng, Siyuan Zhuang, Zhanghao Wu, Yonghao Zhuang, Zi Lin, Zhuohan Li, Dacheng Li, Eric Xing, et al. Judging llm-as-a-judge with mt-bench and chatbot arena. *arXiv preprint arXiv:2306.05685*, 2023.

A1 OVERALL ALGORITHM

The comprehensive training algorithm of OmniQuant is illustrated in Algorithm 1. We employ a block-wise calibration strategy comprising three steps: initialization of learnable parameters (Lines 4-5), training these learnable parameters (Lines 6-15), transforming the model with learned parameters, and then quantization (Lines 16-18). The OmniQuant algorithm finds the optimal transformation to enhance the quantization compatibility of the LLM model. Additionally, due to the elegant design, OmniQuant can achieve rapid convergence using a small calibration dataset.

Algorithm 1 Overall algorithm of OmniQuant.

Input: calibration dataset \mathbf{X} , pre-trained LLM model \mathcal{M}

Output: quantized model.

```

1:  $\mathbf{X}_{fp} = \mathbf{X}_q = \mathbf{X}$  ▷ init inputs of full-precision and quantized models.
2: for  $\mathcal{B}_i$  in  $\mathcal{M}$  do ▷ block-wise calibration
3:    $\mathbf{X}_{fp} = \mathcal{B}_i(\mathbf{X}_{fp})$  ▷ update the input of full-precision model
4:   init learnable weight clipping parameters  $\Theta_1$ 
5:   init learnable equivalent transformation  $\Theta_2$ 
6:   for k in epochs do:
7:     for  $(\mathbf{x}_q, \mathbf{x}_{fp})$  in  $(\mathbf{X}_q, \mathbf{X}_{fp})$  do
8:        $\mathcal{B}'_i = \text{LET}(\mathcal{B}_i, \Theta_2)$  ▷ With Eq.(3), Eq.(5)
9:        $\mathcal{B}'_i = \text{Quantization\_with\_LWC}(\mathcal{B}'_i, \Theta_1)$  ▷ With Eq.(2)
10:       $\mathbf{x}'_q = \mathcal{B}'_i(\mathbf{x}_q)$ 
11:      loss =  $\|\mathbf{x}_{fp} - \mathbf{x}'_q\|^2$  ▷ With Eq.(1)
12:      loss.backward()
13:      update  $\Theta_1$  and  $\Theta_2$  through gradient
14:     end for
15:   end for
16:    $\mathcal{B}_i = \text{LET}(\mathcal{B}_i, \Theta_2)$ 
17:    $\mathcal{B}_i = \text{Quantization\_with\_LWC}(\mathcal{B}_i, \Theta_1)$  ▷ obtain the quantized block
18:    $\mathbf{X}_q = \mathcal{B}_i(\mathbf{X}_q)$  ▷ update the input of quantized model
19: end for
20: return quantized model  $\mathcal{M}$ 

```

A2 TRAINING TIME

As shown in Table A1, we report the training time of the proposed OmniQuant within the LLaMA family. Note that for LLaMA, we only activate learnable weight clipping for weight-only quantization. Therefore, the training time for weight-only quantization is shorter relative to weight-activation quantization, given the fewer learnable parameters involved. While our proposed method necessitates a training time that is approximately $5\times$ greater than GPTQ, it remains markedly faster than QAT methods, which demand hundreds of GPU hours.

Table A1: Omniquant runtime on LLaMA family. The time correspond to training 128 2048-tokes segment over 20 epochs and a batch size of 1 on a single NVIDIA A100-80G.

LLaMA	7B	13B	30B	65B
weight-only	1.1h	2.2h	4.5h	8.9h
weight-activation	1.6h	3.3h	7.3h	14.4h

LLaMA-7B / $l_1 \downarrow$	$\ \mathbf{W} - \mathbf{W}_q\ $		$\ \mathbf{X} - \mathbf{X}_q\ $	
	w/o LWC	w/ LWC	w/o LWC	w/ LWC
quantization				
W2A16g128	0.0089	0.0082	3.24	1.36
W2A16g64	0.0098	0.0086	3.51	1.44
W3A16	0.0062	0.0044	2.80	1.05
W3A16g128	0.0042	0.0040	1.37	0.79
W4A16	0.0028	0.0024	0.98	0.61
W4A16g128	0.0020	0.0019	0.68	0.47

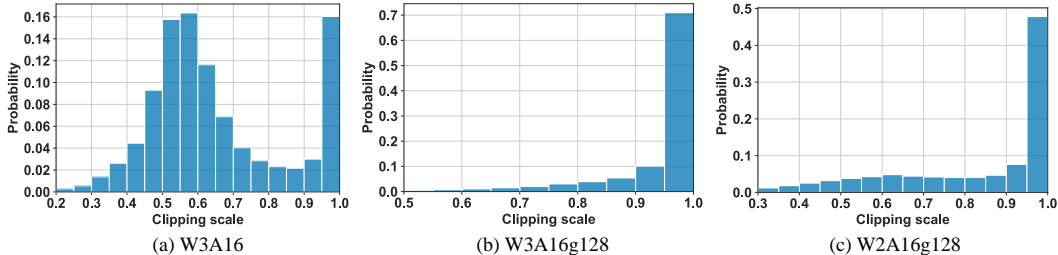
Table A2: l_1 distance between quantized model and full-precision model. $\|\mathbf{W} - \mathbf{W}_q\|$ indicates the average l_1 distance between quantized weight and full-precision weight. $\|\mathbf{X} - \mathbf{X}_q\|$ denotes the l_1 distance between the output of last transformer block.

Figure A1: Visualization of learned clipping scale in different quantization settings in LLaMA-7B.

A3 PERFORMANCE ANALYSIS

In this section, we investigate the internal mechanism of learnable weight clipping and learnable equivalent transformation respectively. Further, we show that with OmniQuant, 3-bit and 4-bit achieve similar trade-off between model bits and perplexity.

Learnable weight clipping. In addition to perplexity and accuracy, the quality of a quantization method can intuitively be evaluated by calculating the distance between quantized models and their full-precision counterparts. This is demonstrated in Table A2, where we detail the l_1 distance of weights and activations for LLaMA-7B’s weight-only quantization. We can observe that the proposed Learned Weight Clipping (LWC) substantially decreases the l_1 distance for both weights and activations. It’s noteworthy that, in certain instances, the l_1 distance for quantized models without LWC is similar to that of those utilizing LWC. However, models incorporating LWC exhibit markedly lower activation l_1 distances. This observation underpins the argument that LWC can effectively balance quantization precision between outlier and regular values.

Additionally, we illustrate the distribution of the learned clipping scale (γ and β) as delineated in Eq. (2) in Figure A1. It is apparent that LWC can learn different clippings for diverse quantization configurations. For instance, with per-channel weight quantization W3A16 as depicted in Figure A1(a), the learned clipping scale showcases a normal distribution. This suggests that approximately half of the outliers are being clipped. In the case of group-wise quantization, the learned clipping scale exhibits a long-tailed distribution, implying that most quantized groups are associated with minimal clipping. Note that lower bits exhibit more pronounced clipping. For example, W2A16g128 possesses a 50% clipping scale larger than 0.95, whereas, in W3A16g128, this percentage rises to 70%.

Learnable equivalent transformation Figure A2 provides visualizations of the intermediate activation in the linear layer. It is apparent that several outlier channels in the original activation (Figure A2(a)) possess significantly larger magnitudes compared to the regular channels, thereby creating an incompatibility with activation quantization. Although SmoothQuant mitigates this issue to some degree, such as reducing the outlier magnitude from 70 to 2, Figure A2(b) reveals that the magnitude of outlier channels still remains notably larger than that of other regular channels after SmoothQuant. This phenomenon can be attributed to SmoothQuant’s heuristic approach in deriving channel-wise scaling, which inevitably makes it challenging to discover an optimal solution. The impact of the proposed LET is depicted in Figure A2(c). It is noteworthy that the magnitude disparity between the outlier and regular channels is markedly diminished. This homogenization of the activation distribution, facilitated by the LET, empowers OmniQuant to efficiently steer the weight-activation quantization towards a low-bit scheme.

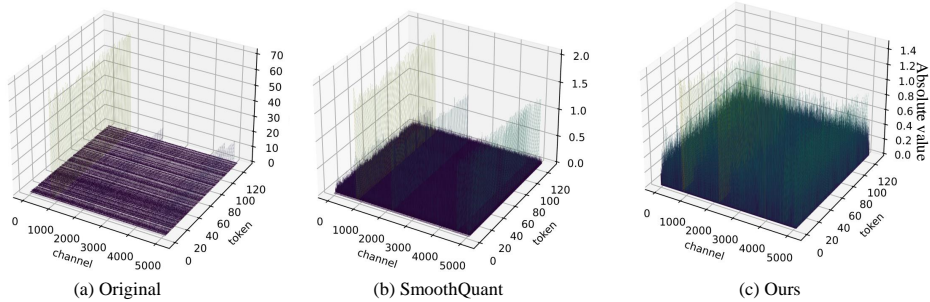


Figure A2: Visualization of activation of a linear layer in OPT-13B. (a) Original activation. (b) Activation after SmoothQuant. (c) Activation after proposed learnable equivalent transformation. Similar phenomena can be observed in different layers and different models.

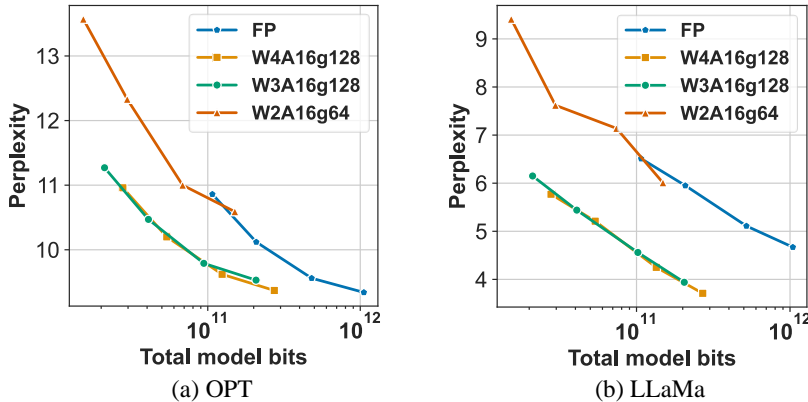


Figure A3: Bit-level scaling laws for perplexity.

Scaling laws. Quantization serves as a potent strategy to curtail the total model bits, thereby facilitating the deployment of LLMs on edge or consumer devices with restricted memory. However, the total model bits are contingent on both the number of parameters within the original model and the quantization bits. Therefore, given a model bits constraint, the challenge arises: how does one optimally determine the number of parameters for the full-precision model and the quantization bits? Tim Dettmers (Dettmers & Zettlemoyer (2023)) demonstrated that 4-bit quantization establishes a universally optimal balance between the total model bits and zero-shot accuracy. Nonetheless, in this study, as shown in Figure A3, we would like to claim that OmniQuant can make 3-bit quantization achieve comparable performance like 4-bit quantization in the trade off between model bits and perplexity.

A4 COMPARISONS WITH CLIPPING-BASED METHOD

In this paper, we proposed a novel method, learnable weight clipping (LWC), designed to adaptively determine the weight clipping threshold. LWC sets the threshold by scaling the original minimum and maximum values to delineate the solution space. We compare LWC against existing clipping-based methods: PACT and LSQ. While PACT directly determines the clipping threshold, LSQ focuses on the direct derivation of the scaling factor and zero-point. Both PACT and LSQ were initially formulated as QAT methods, accounting for both weight and activation clipping. For an equitable comparison, our examination is restricted to weight clipping. We integrated PACT and LSQ into our optimization pipeline in lieu of LWC. Table A3 illustrates that while PACT and LSQ enhance the performance of weight-only quantization in comparison to MinMax quantization, their efficacy diminishes in the weight-activation quantization setting. This decline can be attributed to the proposed LET during activation quantization, which alters the weight distribution in each training iteration, undermining the convergence of both LSQ and PACT. In contrast, LWC defines relative scaling values instead of absolute metrics, making it proficient in handling changes in weight distribution.

Table A3: WikiText2 perplexity of clipping-based quantization methods. For a fair comparison, we reproduce LSQ and PACT by replacing LWC in our pipeline with them.

Method	Perplexity	
	W3A16	W4A4
LLaMA-7B/PPL↓		
FP	5.68	
MinMax	25.73	14.49
PACT (Choi et al. (2018))	6.95	18.25
LSQ (Esser et al. (2019))	6.63	15.03
LWC (Ours)	6.47	11.26

A5 MORE ABLATION STUDIES

Table A4: **Ablation of learnable equivalent transformation.** WikiText2 perplexity1 is reported in this table.

Method	PPL↓	LLaMA-13B		OPT-13B	
		W4A4	W3A16	W4A4	W3A16
LWC+LET		11.86	5.65	11.65	10.87
LET -shifting		12.37	5.65	13.64	10.87
LET -attention		11.98	5.65	11.79	10.87

Table A5: **Ablation of training time.** We train LLaMA-7B with different quantization configuration on 128 2048-tokens segments from WikiText2 over various epochs. ‘0’ indicates only initialization without fine-tuning. Wikitext perplexity is reported in this table.

Epochs	W4A16	W3A16	W2A16	W6A6	W4A4
0	6.29	24.04	1.1e5	6.16	33.93
10	5.87	6.51	27.49	5.96	12.04
20	5.85	6.49	17.46	5.95	11.26
40	5.86	6.47	15.47	5.95	11.23
80	-	-	14.77	-	-

Design choices of learnable equivalent transformation. In comparison to the equivalent transformation incorporated in SmoothQuant (Xiao et al. (2023)), our approach additionally implements channel-wise shifting and attention transformation. The effects of these innovations are evaluated in Table,A4. We can observe that both modifications enhance the performance of weight-activation quantization. However, the incremental benefit from the equivalent transformation in the attention operation is comparatively minor. This discrepancy is primarily due to the majority of outliers existing in the output of the normalization layer while being less prevalent in the $Q/K/V$ matrix.

Table A6: Ablation of calibration dataset.

LLaMA-7B/PPL↓	W3A16		W4A4	
	WikiText2	C4	WikiText2	C4
Calibration Dataset				
WikiText2	6.47	8.19	11.23	14.61
C4	6.67	8.13	12.17	14.24
Pile	6.69	8.17	12.04	14.22
Variance	0.009	0.0006	0.17	0.03

Table A7: Ablation of sample number of calibration dataset.

LLaMA-7B/PPL↓	W3A16		W4A4	
	WikiText2	C4	WikiText2	C4
Sample Number				
16	6.47	8.18	11.56	14.84
32	6.47	8.18	11.48	14.80
64	6.48	8.19	11.40	14.57
128	6.47	8.19	11.23	14.61
256	6.46	8.19	11.41	14.90

Training Time As illustrated in Table A5, LLaMA-7B was trained across various epochs to determine the optimal convergence time. Most quantization configurations converge within 20 epochs, with the exception of W2A16, which necessitates 80 epochs. Consequently, we establish a training epoch of 20 for all configurations, except for W2A16, for which we set it to 40 in consideration of the training time.

Training Data OmniQuant utilizes gradient optimization on constrained calibration datasets, sourced from WikiText2 and comprising 128 segments with 2048 tokens each. This prompts concerns about potential overfitting to the calibration dataset. To explore this, we evaluated the calibration dataset’s influence using two other datasets: Pile (Gao et al. (2020)) and c4 (Raffel et al. (2020)). As depicted in Table A6, the variance in perplexity across diverse calibration datasets is marginal, fluctuating between 0.0006 and 0.17. This underscores OmniQuant’s robustness concerning calibration set distribution. Furthermore, the data efficiency of OmniQuant was gauged by modulating the number of training samples, as presented in Table A7. Remarkably, OmniQuant converges with as few as 16 samples. Our selection of 128 samples aligns with established practices in prior works (Frantar et al. (2022); Lin et al. (2023)).

A6 FULL RESULTS

In this section, we provide a comprehensive presentation of our results across various datasets to complement the main paper. Specifically, the results include:

- C4 perplexity with weight-only quantization in the LLaMA families (Table A8).
- PTB perplexity with weight-only quantization in OPT families (Table A10).
- C4 perplexity with weight-only quantization in OPT families (Table A11).
- WikiText2 perplexity for weight-activation quantization in the LLaMA families (Table A12).
- C4 perplexity for weight-activation quantization in the LLaMA families (Table A13).
- WikiText2/PTB/C4 perplexity for weight-activation quantization in the LLaMA families (Table A14).

Table A8: C4 perplexity of Weight-only quantization Results in LLaMA-1 and LLaMA-2 Models Continue of Table 1.

LLaMA1&2 / PPL↓		1-7B	1-13B	1-30B	1-65B	2-7B	2-13B	2-70B
FP16	-	7.08	6.61	5.98	5.62	6.97	6.46	5.70
W2A16	RTN	1.3e5	5.6e4	2.7e4	2.2e4	4.8e4	7.2e4	2.4e4
	GPTQ	689.13	2.5e3	169.80	40.58	NAN	323.12	48.82
	OmniQuant	24.89	18.31	13.89	10.77	90.64	26.76	12.28
W2A16 g128	RTN	1.0e3	447.64	99.45	17.15	4.9e3	139.65	42.13
	GPTQ	27.71	15.29	11.93	11.99	33.70	20.97	NAN
	AWQ	1.9e5	2.3e5	2.4e5	7.5e4	1.7e5	9.4e4	-
	OmniQuant	13.89	11.02	9.85	8.26	17.40	11.87	9.16
W2A16 g64	RTN	151.43	76.00	30.07	11.34	475.35	28.69	13.43
	GPTQ	17.71	11.70	9.92	10.07	19.40	12.48	NAN
	AWQ	2.8e5	2.2e5	2.3e5	7.4e4	1.6e5	9.5e4	-
	OmniQuant	12.29	9.97	9.02	7.78	13.77	10.47	8.20
W3A16	RTN	28.26	13.22	28.66	12.79	402.35	12.51	10.02
	GPTQ	9.49	8.16	7.29	6.71	9.81	8.02	6.57
	AWQ	13.26	9.13	12.67	7.11	23.85	13.07	-
	OmniQuant	8.19	7.32	6.57	6.07	8.65	7.44	6.06
W3A16 g128	RTN	8.62	7.49	6.58	6.10	8.40	7.18	6.02
	GPTQ	7.85	7.10	6.47	6.00	7.89	7.00	5.85
	AWQ	7.92	7.07	6.37	5.94	7.84	6.94	-
	OmniQuant	7.34	6.76	6.11	5.73	7.35	6.65	5.86
W4A16	RTN	7.93	6.98	6.34	5.85	7.71	6.83	5.79
	GPTQ	7.43	6.84	6.20	5.80	7.37	6.70	5.67
	AWQ	7.52	6.86	6.17	5.77	7.68	6.74	-
	OmniQuant	7.34	6.76	6.11	5.73	7.35	6.65	5.65
W4A16 g128	RTN	7.37	6.69	6.06	5.69	7.24	6.58	5.63
	GPTQ	7.21	6.69	6.06	5.69	7.12	6.56	5.58
	AWQ	7.21	6.70	6.05	5.68	7.13	6.56	-
	OmniQuant	7.21	6.69	6.06	5.68	7.12	6.56	5.58

Table A9: WikiText2 perplexity of Weight-only quantization Results in OPT Models.

OPT / PPL↓		125M	1.3B	2.7B	6.7B	13B	30B	66B
FP16	-	27.65	14.63	12.47	10.86	10.12	9.56	9.34
W2A16 g128	RTN	7.2e3	1.3e4	5.7e4	7.8e3	7.6e4	1.3e4	3.6e5
	GPTQ	597.66	115.16	61.59	20.18	21.36	12.71	82.10
	AWQ	251.84	47.97	28.50	16.20	14.32	12.31	14.54
	OmniQuant	75.43	23.95	18.13	14.43	12.94	11.39	30.84
W2A16 g64	RTN	7.0e3	1.0e4	19.3e4	7.6e3	1.8e4	8.2e3	1.1e4
	GPTQ	204.40	49.58	29.37	16.81	16.65	11.87	356.01
	AWQ	124.18	29.78	20.64	14.63	13.28	11.59	12.74
	OmniQuant	62.56	21.40	16.76	13.57	12.33	11.00	10.59
W3A16	RTN	1.2e3	1.3e4	1.6e4	6.5e3	4.6e3	1.5e3	6.1e3
	GPTQ	53.05	21.17	16.83	15.09	11.73	10.30	14.42
	AWQ	69.43	28.01	263.10	15.13	20.09	35.74	4.5e3
	OmniQuant	35.66	16.68	13.80	11.65	10.87	10.00	9.83
W3A16 g128	RTN	51.22	119.00	297.98	23.54	46.03	18.80	136.89w
	GPTQ	39.24	16.47	13.69	11.65	10.35	9.73	10.96
	AWQ	36.74	16.32	13.58	11.41	10.68	9.85	9.60
	OmniQuant	32.25	15.72	13.18	11.27	10.47	9.79	9.53
W4A16	RTN	37.28	48.17	16.92	12.10	11.32	10.97	110
	GPTQ	31.43	15.56	12.82	11.41	10.31	9.63	9.55
	AWQ	32.28	15.49	12.93	11.30	10.39	9.77	9.61
	OmniQuant	29.45	15.04	12.76	11.03	10.30	9.65	9.65
W4A16 g128	RTN	30.47	15.29	13.02	11.15	10.30	9.94	9.65
	GPTQ	29.81	14.89	12.52	10.93	10.17	9.58	9.34
	AWQ	29.15	14.94	12.74	10.93	10.21	9.59	9.40
	OmniQuant	28.86	14.88	12.65	10.96	10.20	9.62	9.37

Table A10: PTB perplexity of Weight-only quantization Results in OPT Models.

OPT / PPL↓		125M	1.3B	2.7B	6.7B	13B	30B	66B
FP16	-	32.54	16.96	15.11	13.08	12.33	11.84	11.36
W2A16 g128	RTN	4.6e3	7.1e3	2.5e4	5.7e3	3.0e4	6.2e3	1.4e5
	GPTQ	655.17	130.88	61.36	25.24	20.46	15.15	323.23
	AWQ	263.88	71.87	43.15	19.49	17.61	14.92	19.33
	OmniQuant	126.49	34.33	25.28	18.92	16.74	14.51	139.17
W2A16 g64	RTN	5.1e3	9.4e3	7.7e4	6.1e3	8.2e3	4.1e3	6.2e3
	GPTQ	245.28	55.61	36.12	19.45	17.02	14.05	88.92
	AWQ	143.18	41.19	25.08	18.00	15.83	14.92	15.72
	OmniQuant	112.10	30.36	22.63	17.58	15.70	13.98	13.51
W3A16	RTN	1.2e3	1.1e4	1.0e4	5.2e3	3.6e3	1.4e3	3.6e3
	GPTQ	34.05	27.39	15.94	13.75	13.71	12.54	21.16
	AWQ	80.73	33.20	224.11	18.46	35.45	66.68	3.4e3
	OmniQuant	40.76	19.06	16.29	13.77	12.96	12.19	11.71
W3A16 g128	RTN	64.67	222.13	337.75	39.90	65.33	34.27	309.69
	GPTQ	45.17	19.90	17.06	14.24	12.84	12.54	13.27
	AWQ	44.07	19.59	16.52	13.98	12.87	66.68	3.4e3
	OmniQuant	45.29	20.42	17.08	14.23	13.49	12.54	12.06
W4A16	RTN	44.98	33.63	22.23	16.05	15.40	14.17	274.23
	GPTQ	37.75	18.23	15.94	13.75	12.58	11.98	11.58
	AWQ	38.74	18.35	15.70	13.59	12.72	12.06	11.58
	OmniQuant	34.94	17.80	15.52	13.41	12.62	11.95	11.86
W4A16 g128	RTN	36.50	33.63	22.23	16.05	15.40	14.17	11.79
	GPTQ	35.48	17.41	15.42	13.21	12.42	11.89	11.51
	AWQ	34.95	17.46	15.33	13.28	12.46	11.90	11.43
	OmniQuant	34.28	17.40	15.28	13.25	12.46	11.94	11.40

Table A11: C4 perplexity of Weight-only quantization Results in OPT Models.

OPT / PPL↓		125M	1.3B	2.7B	6.7B	13B	30B	66B
FP16	-	24.60	14.72	13.16	11.74	11.19	10.69	10.28
W2A16 g128	RTN	5.0e3	7.7e3	3.8e4	5.2e3	2.8e4	6.5e3	2.6e5
	GPTQ	597.66	60.88	33.83	18.55	16.34	12.89	598.81
	AWQ	168.35	38.38	26.41	16.48	14.73	12.98	15.42
	OmniQuant	80.10	27.33	21.11	16.67	14.92	13.12	73.83
W2A16 g64	RTN	3.9e3	7.3e3	1.2e5	6.3e3	7.5e3	4.0e3	8.4e3
	GPTQ	133.51	31.31	23.23	16.24	14.48	12.24	58.60
	AWQ	90.19	27.34	20.01	15.20	13.90	12.43	13.31
	OmniQuant	64.01	23.71	19.16	15.44	14.16	12.80	12.13
W3A16	RTN	722.83	6.1e3	1.2e4	5.8e3	3.3e3	1.4e3	3.6e3
	GPTQ	37.75	19.45	13.75	15.67	12.28	11.34	13.68
	AWQ	55.73	24.56	154.49	15.84	23.71	55.01	3.8e3
	OmniQuant	32.17	17.10	14.93	12.78	12.13	11.37	10.82
W3A16 g128	RTN	40.13	126.47	372.23	32.56	44.12	25.70	286.87
	GPTQ	30.08	16.47	14.54	12.48	11.58	10.91	11.35
	AWQ	30.39	16.27	14.19	12.30	11.61	10.96	10.53
	OmniQuant	29.34	16.11	14.15	12.31	11.63	10.98	10.51
W4A16	RTN	31.58	24.68	17.61	13.38	12.35	11.90	249.54
	GPTQ	27.12	15.57	13.75	12.15	11.36	10.80	10.50
	AWQ	27.64	15.65	13.71	12.04	11.42	10.83	10.41
	OmniQuant	26.36	15.28	13.58	11.97	11.41	10.80	10.63
W4A16 g128	RTN	26.79	15.71	13.79	12.31	11.51	10.94	10.54
	GPTQ	25.96	15.05	13.40	11.87	11.26	10.74	10.37
	AWQ	25.90	15.04	13.39	11.87	11.28	10.75	10.34
	OmniQuant	25.63	15.03	13.38	11.85	11.29	10.75	10.33

Table A12: **WikiText2 perplexity of weight-activation quantization Results in LLaMA-1 and LLaMA-2 Models** Continue of Table 2.

LLaMA1&2 / PPL↓		1-7B	1-13B	1-30B	1-65B	2-7B	2-13B
FP16	-	5.68	5.09	4.10	3.53	5.47	4.88
W6A6	SmoothQuant	6.03	5.42	4.55	3.88	6.20	5.18
	OmniQuant	5.96	5.28	4.38	3.75	5.87	5.14
W4A4	SmoothQuant	25.25	40.05	192.40	275.53	83.12	35.88
	OmniQuant	11.26	10.87	10.33	9.17	14.61	12.30

Table A13: **C4 perplexity of weight-activation quantization Results in LLaMA-1 and LLaMA-2 Models.** Continue of Table 2.

LLaMA1&2 / PPL↓		1-7B	1-13B	1-30B	1-65B	2-7B	2-13B
FP16	-	7.08	6.61	5.98	5.62	6.97	6.46
W6A6	SmoothQuant	7.47	6.97	6.34	5.99	7.76	6.76
	OmniQuant	7.43	6.84	6.22	5.82	7.48	6.74
W4A4	SmoothQuant	32.32	47.18	122.38	244.35	77.27	43.19
	OmniQuant	14.51	13.78	12.49	11.28	18.39	14.55

Table A14: **Weight-activation quantization results of OPT Models.** We report perplexity on three datasets: WikiText2 (WIKI), Pen Treebank (PT), and C4. RPTQ indicates the data from RPTQ (Yuan et al. (2023)) paper, which keeps the output of LN and SoftMax as 8-bit. RPTQ* represents reproducing RPTQ with our setting that quantizes all activation into low-bit except keeping the softmax output at full precision.

OPT / PPL↓		OPT-6.7b			OPT-13b			OPT-30b			OPT-66b		
Task		WIKI	PT	C4	WIKI	PT	C4	WIKI	PT	C4	WIKI	PT	C4
FP16	-	10.86	13.09	11.74	10.13	12.34	11.20	9.56	11.84	10.69	9.34	11.36	10.28
W6A6	SmoothQuant	11.34	13.82	12.14	10.56	12.76	11.40	9.67	12.01	10.81	10.72	13.25	11.60
	RPTQ	11.19	13.98	12.08	11.00	15.23	11.68	10.22	14.95	11.73	9.45	13.03	10.62
	RPTQ*	10.96	13.24	11.86	10.25	12.60	11.31	9.60	12.23	10.83	9.48	12.61	10.39
	OmniQuant	10.96	13.20	11.81	10.21	12.47	11.27	9.62	11.92	10.76	9.42	11.42	10.32
W4A4	SmoothQuant	1.8e4	1.4e4	1.5e4	7.4e3	6.5e3	5.6e3	1.2e4	7.8e3	8.3e3	2.2e5	1.0e5	1.8e5
	RPTQ	12.00	15.17	12.85	12.74	15.76	14.71	11.15	14.11	13.48	12.23	18.87	15.93
	RPTQ*	17.83	25.10	19.91	16.45	23.01	16.80	11.50	14.87	12.81	11.16	13.73	11.78
	OmniQuant	12.24	15.54	13.56	11.65	15.89	13.46	10.60	13.75	11.89	10.29	13.19	11.35